

Alignment film abrasion caused by rubbing

Hirokazu Kamada^a, Ikuo Ihara^b, Hong Dae Kim^{a,c}, Tadachika Nakayama^a, Munehiro Kimura^{a*}, and Tadashi Akahane^a

^aDepartment of Electrical Engineering, Nagaoka University of Technology, 1603-1 Kamitomioka, Nagaoka, Niigata Prefecture 940-2188, Japan; ^bDepartment of Mechanical Engineering, Nagaoka University of Technology, 1603-1 Kamitomioka, Nagaoka, Niigata Prefecture 940-2188, Japan; ^cGreen Technology Center, Korea Institute of Industrial Technology, 421 Daun-dong, Ulsan 681-802, South Korea

(Received 3 June 2011; Revised 22 August 2011; Accepted 26 August 2011)

The alignment film abrasion caused by the rubbing process was quantitatively evaluated via atomic-force microscopy (AFM). First, a patterned alignment film structure, which was molded through the imprint method, was artificially formed. Then, the surface topography of the alignment film was evaluated via AFM after rubbing, and the degree of abrasion of the alignment film was estimated by subtracting the value after rubbing from the value before rubbing. It was recognized that the degree of abrasion increased with an increase in the rubbing strength. The relationship between the number of rubbing cycles and the degree of abrasion of the alignment film was also estimated.

Keywords: rubbing; polyimide; rubbing scratch; abrasion; Vickers hardness

1. Introduction

One hundred years have passed since the first report on the mechanical rubbing process was released by Mauquin [1]. Nowadays, the rubbing process is used worldwide as a manufacturing process for liquid crystal display (LCD) because of its high productivity. The relative friction between the rubbing cloth and the alignment film induces anisotropy of the polymer film that coats the glass substrate. As a result, the rubbed polymer film acts as an alignment film for liquid crystal (LC) molecules. Polyimides (PIs) are widely used as LC alignment films in the mass production of LCD because of their advantageous properties such as excellent optical transparency, adhesion, heat resistance, dimensional stability, and insulation [2–4]. Among the problems caused by the rubbing process are the so-called ‘rubbing scratches’ [5–9], which deteriorate the transmittance attenuation at the black state [10,11]. Excess friction damages the surface of the alignment film, and light leakage around the scratched alignment surface, which reduces the contrast ratio of an LCD, is caused by the induced molecular-alignment defect. It is assumed that the cause of the molecular-alignment defect is the fact that the alignment film surface was topologically scratched by the rubbing cloth. Generally, evaluations of the surface of the alignment film have been done after the rubbing process, by observing the LC alignment and/or the topology of the alignment film via atomic-force microscopy (AFM) [12,13]. The objects of the investigation of the rubbing effect, however, were

the evaluation of the depth of the scratch groove and its histogram. In other words, it is uncertain whether the surface of the alignment film was just scratched or whether a certain thickness of the alignment film was abraded by the rubbing process. There is a possibility that the alignment film was fairly *uniformly* abraded while the surface roughness was quite small. Zheng et al. [9] reported that as the number of rubbing cycles increases, the number of grooves likewise increases, and the width and peak-to-valley height of the grooves decrease. During rubbing, the peaks in the corrugated surface suffer much higher abrasion rates than the troughs, leading to a reduction in the peak-to-valley height and a decrease in the surface roughness with an increase in the rubbing strength (RS). This result implies that at a certain thickness, the alignment film can be abraded through the rubbing process. In a real case of the active matrix-type LCD panel, an alignment film covering the structure of the thin-film transistor may be more abraded than that covering the plane electrode, which may disturb the uniform LC alignment throughout the pixel. It is difficult, however, to compare the net thickness of the alignment film before and after the rubbing process through optical measurement because the alignment film is fairly thin (<50 nm) and is less than the wavelength of the probing light. Therefore, sufficient measurement accuracy cannot be guaranteed. To evaluate the exact degree of abrasion of the alignment film, it should be prepared as a thickness-known alignment film beforehand. The degree of abrasion can be

*Corresponding author. Email: nutkim@vos.nagaokaut.ac.jp

estimated by using the contact-type profilometer or AFM after the rubbing process.

Nanoimprint lithography (NIL), a novel method of forming a nanopattern, has attracted many researchers' interest because of its low-cost technology and mass production [14–18]. It is expected that a thickness-known alignment film transferred via the imprint technique can be original and that the abrasion loss can be estimated through AFM measurement after the rubbing process. In this paper, the abrasion characteristic was investigated via AFM and the imprint technique, and the relationship between the number of rubbing cycles and abrasion loss was studied.

2. Experiments

In a traditional thermoplastic NIL, a resist polymer film is coated onto the sample substrate. Then, the mold, which has predefined topological patterns covered with an anti-sticking layer, is brought into contact with the resist polymer film. The mold and the resist polymer film are then pressed together under a certain pressure. When the resist polymer is heated up above the glass transition temperature, the pattern on the mold is pressed and replicated into the softened resist polymer. After cooling, the mold is separated from the sample substrate, and the pattern-transferred resist film is left on the substrate. The traditional thermoplastic NIL, however, was not applicable to this study for two reasons: the concentration of the commercially available PI solution is too low to make replication, and a replica cannot be made by using high-concentration PI solution with high elasticity. Therefore, a contrivance is adopted as follows. First, the glass substrate was coated with an appropriate concentration of PI solution and was prebaked for 3 min at 80°C. Second, the mold with predefined topological patterns and the substrate were pressed by approximately 8 kg/cm²; this was maintained for 2 h at the post-baking temperature, to volatilize the solvent and to cause the PI to accumulate between the top of the mold and the substrate surface via capillary action. As a result, a fine PI replica can be obtained. In this sense, this technique is different from the original imprint method, and therefore, the thickness of the PI film cannot be controlled arbitrarily.

Two types of PIs were used for the alignment films in this study: (1) cyclobutane dianhydride and 2,2-bis(4-aminophenoxyphenyl) propane (CBDA/BAPP) (provided by Nissan Chemical Industries Ltd), whose concentration was approximately 15 wt% (diluted with *N*-methyl-2-pyrrolidone) and whose post-baking temperature was 250°C; and (2) PIA-X001 (provided by JNC Petrochem. Co.), a commercially available PI with a different chemical structure from CBDA/BAPP, whose concentration was approximately 50 wt% (diluted with ethylene glycol monomethyl ether) and whose post-baking temperature was 230°C. It is beneficial for the hardness of the PI to be evaluated as a reference. Miyajima et al. [19] reported the

torsional stiffness of PI. In this experiment, the indentation test was performed using a load-controlled indentation tester (ENT-2100, Elionix Inc.) with a Berkovich diamond tip. The loading and displacement resolutions of the indentation tester were 4 nN and 0.06 nm, respectively. The maximum penetration depth of the Berkovich tip in the indentation was about 40 nm, whereas the maximum loading was set at 20 μN. The detailed description of the theory behind the nanoindentation test has been provided in numerous references [20]. The measured Vickers hardness and Young's modulus of CBDA/BAPP were approximately 0.55 and 6.2 GPa, respectively, which are almost similar to the values reported in the previous papers [19,21].

Three types of mold were prepared in the experiment that was conducted in this study. One is the molybdenum (Mo) mold, whose surface has alternate stripe patterns with 30 μm width line and 50 μm width space. This stripe-shaped step imitates the substrate structure for transfective LCD. The others are silicone molds, whose surface has a 0.5 μmϕ dimple pattern, a 2 μmϕ cylinder cluster pattern, or alternate stripe patterns with 1 μm width line and 1 μm width space, respectively. Trichlorosilane diluted 300 times with ethanol was used as an anti-sticking layer. After the molding and post-baking procedure, the mold was slowly separated. Then, the rubbing processing was carried out on the surface of the PI film using a rubbing machine (Joyo Engineering Co., Ltd), as shown in Figure 1. The rubbing cloth used was made of cotton (provided by Kuraray Trading Co., Ltd), which was fastened onto the rotating drum. The total length of the rubbing cloth, which comes in contact with the substrate at a certain point and which is also sometimes called RS parameter, is given by [22]

$$RS = N \cdot l \left(1 + \frac{2\pi rn}{60v} \right), \quad (1)$$

where N is the cumulative number of rubs, l the contact length of the circumference of the rubbing roller, n the rotational speed of the rotating drum, r the radius of the

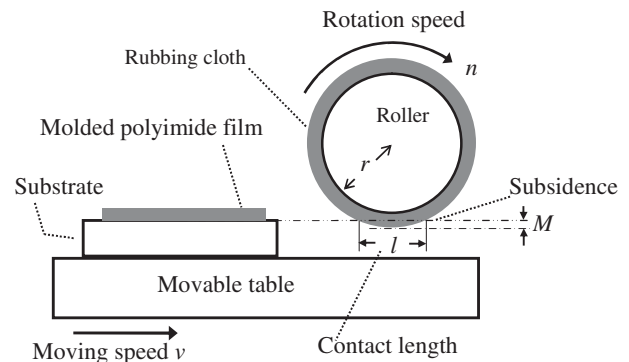


Figure 1. Schematic illustration of the rubbing machine.

drum, and v the moving speed of the movable table, respectively. Drum radius r was 26.15 mm. The PI film sample substrate was placed on the movable table. Before and after the rubbing process, the surface topology of the PI film was observed using an AFM (SPM-9500J2, Shimadzu Co.).

3. Results and discussion

First, to reconfirm the rubbing abrasion phenomenon at the corner edge of the step-shaped PI layer, Figure 2 shows typical AFM images of a stripe-patterned PIA-X001 replica before and after processed rubbing, where the Mo mold was

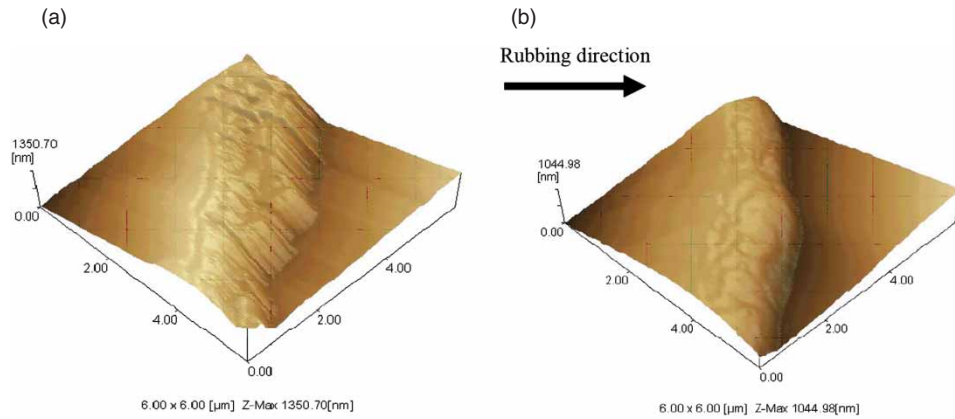


Figure 2. Typical AFM images of the corner edge of the step-shaped PIA-X001 replica: (a) before rubbing and (b) after rubbing.

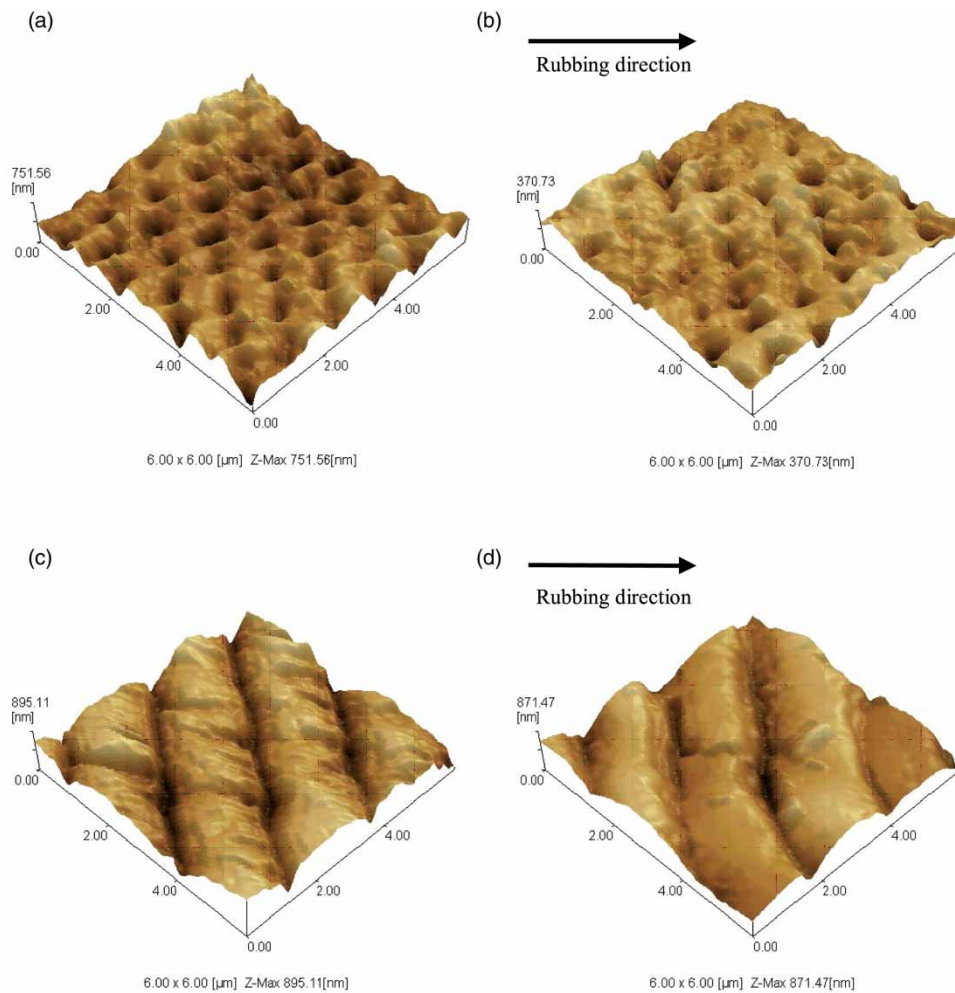


Figure 3. Typical AFM images of the CBDA/BAPP replica: (a) imprinted by dimple mold; (b) imprinted by dimple mold and rubbed; (c) imprinted by stripe mold; and (d) imprinted by stripe mold and rubbed.

used. As for the rubbing conditions, the rotational speed of the rubbing drum n was 500 rpm, the moving speed of the movable table v was 5 mm/s, and the subsidence of the rubbing cloth was 0.5 mm, which are the commonly used values in the manufacturing process for real production. The resultant RS was 2800 nm. As the scanning area of AFM ($< 30 \mu\text{m}^2$) is narrower than the stripe pattern, one side of the corner edge was observed. To compare the replica shapes before and after the rubbing process, inclination correction over the scanned area was not applied to the AFM images. Before the rubbing process (shown in Figure 2a), it was found that the average height of the step was approximately $0.95 \mu\text{m}$. After the rubbing process (shown in Figure 2b), the corner edge of the step-shaped PI layer was worn out and the average height was decreased to approximately $0.63 \mu\text{m}$. This result implies that a certain amount of PI layer was abraded by the friction caused by the rubbing cloth, although PI seems to be much harder than cotton.

Figure 3 represents the typical AFM images of dimple- and stripe-patterned CBDA/BAPP replicas before and after processed rubbing, where the Si mold was used. As for the rubbing conditions, the rotational speed of the rubbing

drum n was 150 rpm, the moving speed of the movable table v was 10 mm/s, and the subsidence of the rubbing cloth was 0.5 mm. The resultant RS was 430 nm. As shown in Figure 3(a) and (c), before the rubbing process, the average depth of the dimple was approximately 122 nm, and the average height of the step was approximately 552 nm. After the rubbing process, it was found that the average undulation decreased to 82 nm (shown in Figure 3b) and 215 nm (shown in Figure 3d). As shown in Figure 3(d), the abrasion phenomenon, in which the corner edge of PI is worn out, is similar to Figure 2(b). The stripe-patterned CBDA/BAPP suffers much higher abrasion rates than the dimple-patterned CBDA/BAPP, and the cause seems to be the difference in structural mechanics of the patterned PIs.

The dependence of the abrasion rate on RS was investigated. Figure 4 shows typical AFM images of the patterned CBDA/BAPP replica before and after processed rubbing, where the Si-cylinder-cluster-patterned mold was used. As for the rubbing conditions, the rotational speed of the rubbing drum n was 150 rpm, the moving speed of the movable table v was 10 mm/s, and the subsidence of the rubbing cloth was 0.5 mm. The resultant RS was 430 nm. After the rubbing process, an AFM image was obtained

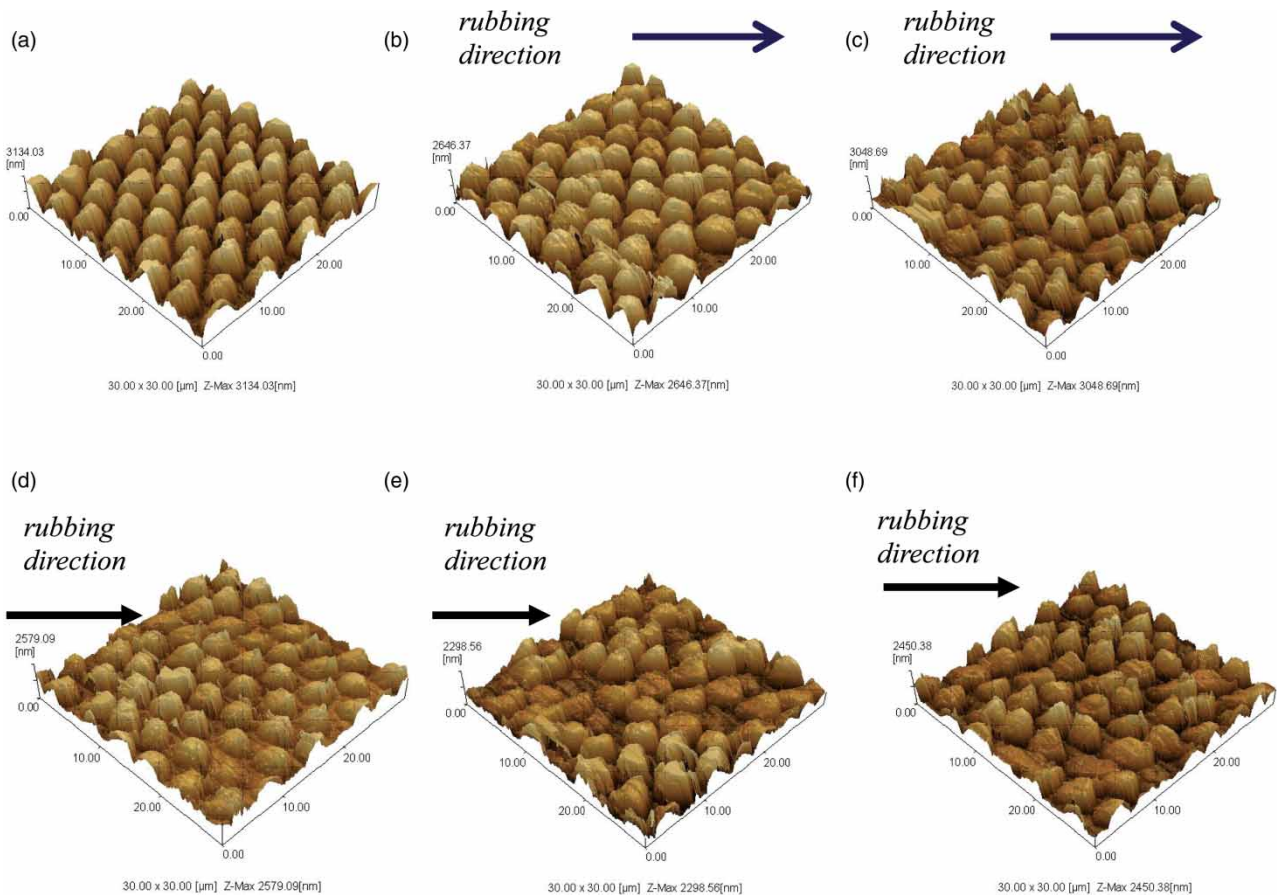


Figure 4. Typical AFM images of the CBDA/BAPP replica: (a) imprinted by the cylinder-cluster-patterned mold ($N = 0$); (b) imprinted by mold and rubbed once ($N = 1$); (c) rubbed twice ($N = 2$); (d) rubbed three times ($N = 3$); (e) rubbed four times ($N = 4$); and (f) rubbed five times ($N = 5$).

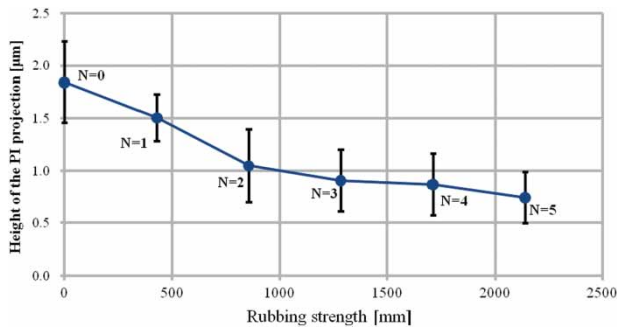


Figure 5. Dependence of the abrasion rate of the rubbed CBDA/BAPP on the RS. N represents the number of rubbing cycles.

once (Figure 4, $N = 1$). Then the second rubbing process was done, which meant RS = 860 mm. After that, another AFM image was obtained (Figure 4, $N = 2$); the third rubbing process was done and an AFM image was obtained (Figure 4, $N = 3$). The rubbing and AFM observation were repeated up to five times. It is clearly shown that the molded CBDA/BAPP was worn out by the rubbing process. Especially, the peaks of the projection were worn out. From the experiment represented by Figure 4, Figure 5 shows the height of the projection of molded CBDA/BAPP after the rubbing process, which represents the dependence of the abrasion rate on RS. It was found that the abrasion rate monotonously increases with increasing RS. From these experimental results, it can be concluded that a certain thickness of the PI alignment film was abraded by the rubbing process and that the peak or edge region of the PI surface suffers much higher abrasion rates than the trough regions.

4. Summary

The surface abrasion phenomenon caused by the conventional rubbing process was experimentally estimated by means of the imprint technique and surface topological observation. The purpose of this method is to enable the measurement of the net abrasion loss, other than the surface roughness. Although the Vickers hardness of a PI film is relatively high enough, it was confirmed that the surface of PI was abraded by the rubbing cloth. It was also confirmed that the number of rubbing cycles and the RS have a correlation with the abrasion loss. These phenomena have to be called 'rubbing abrasion' rather than 'rubbing scratch,' which is a serious problem for the LCD panel whose interior has a PI surface with a terrace structure. In this paper, the cumulative number of rubs has been changed instead of changing the contact length, rotational speed, and translational speed. As reported by Uchida *et al.* [23], the responsibility of each rubbing parameter in Equation (1) may be different. To find the optimum rubbing conditions by which an appropriate anisotropy of the alignment film is given without rubbing

scratches, further investigation is required by changing the rubbing parameters.

Acknowledgements

The authors thank Merck Ltd Japan, JNC Petrochem Co., and Nissan Chemical Industries Ltd for providing them with LC and PI materials.

References

- [1] C. Mauguin, *Bull. Soc. fr. Miner.* **34**, 71 (1911).
- [2] B. Bahadur, *Liquid Crystals: Applications and Uses* (World Scientific, Singapore, 1990), Vol. 1, Chap. 7.
- [3] M.K. Ghosh and K.L. Mittal, *Polyimides: Fundamentals and Applications* (Marcel Dekker, New York, NY, 1996), Chap. 24.
- [4] S.W. Lee, S.J. Lee, S.G. Hahm, T.J. Lee, B. Lee, B. Chae, S.B. Kim, J.C. Jung, W.C. Zin, B.H. Sohn, and M. Ree, *Macromolecules* **38**, 4331 (2005).
- [5] N.A.J.M. van Aerle, *J. Soc. Inf. Disp.* **2**, 41 (1994).
- [6] K.-Y. Han and T. Uchida, *J. Soc. Inf. Disp.* **3**, 15 (1995).
- [7] D.-H. Chung, Y. Takanishi, K. Ishikawa, H. Takezoe, B. Park, Y. Jung, H.-K. Hwang, S. Lee, K.-J. Han, and S.-H. Jang, *Jpn. J. Appl. Phys.* **39**, L185 (2000).
- [8] H.-K. Hong and C.-R. Seo, *Jpn. J. Appl. Phys.* **43**, 7639 (2004).
- [9] W. Zheng, C.-H. Lu, and Y.-C. Ye, *Jpn. J. Appl. Phys.* **47**, 1651 (2008).
- [10] H. Tabira, T. Inoue, Y. Yahagi, H. Imayama, and M. Morimoto, *J. Soc. Inf. Disp.* **10**, 329 (2002).
- [11] K.-M. Son, S.-K. Kim, J.-W. Lee, S.-Y. Noh, J.-P. Kim, S.-R. Park, J.-Y. Yang, M.-S. Yang, I.-B. Kang, and I.-J. Chung, *J. Soc. Inf. Disp.* **18**, 37 (2010).
- [12] H. Seki, Y. Masuda, and T. Uchida, *Mol. Cryst. Liq. Cryst.* **282**, 323 (1996).
- [13] M.P. Mahajan and C. Rosenblatt, *J. Appl. Phys.* **83**, 7649 (1998).
- [14] S.Y. Chou, P.R. Krauss, and P.J. Renstrom, *Appl. Phys. Lett.* **67**, 3114 (1995).
- [15] R. Ozaki, T. Shinpo, K. Yoshino, M. Ozaki, and H. Moritake, *Appl. Phys. Express* **1**, 012003 (2008).
- [16] Y. Yi, G. Lombardo, N. Ashby, R. Barberi, J.E. Maclennan, and N.A. Clark, *Phys. Rev. E* **79**, 041701 (2009).
- [17] J.-Y. Chun and D.-S. Seo, *Jpn. J. Appl. Phys.* **49**, 040210 (2010).
- [18] H. Takahashi, T. Sakamoto, and H. Okada, *J. Appl. Phys.* **108**, 113529 (2010).
- [19] H. Miyajima, T. Arikawa, T. Hidaka, K. Tokuda, and K. Matsumoto, *Sens. Actuators A* **117**, 341 (2005).
- [20] W.C. Oliver and G.M. Pharr, *J. Mater. Res.* **7**, 1564 (1992).
- [21] C. Lee, N.P. Iyer, and H. Han, *J. Polym. Sci. B* **42**, 2202 (2004).
- [22] Y. Sato, K. Sato, and T. Uchida, *Jpn. J. Appl. Phys.* **31**, L579 (1992).
- [23] T. Uchida, E.S. Lee, and T. Miyashita, *Tech. Rep. IEICE (EID94-86)*, **94**, 327, 47 (1994) (in Japanese).